Inorg. Chem. **2003**, *42*, 5126–5134

Ligand Entrapment in Twofold Interpenetrating PtS Matrixes by Metallo-Organic Frameworks

Kalle I. Nättinen[†] **and Kari Rissanen***

Department of Chemistry, University of Jyväskylä, P.O. Box 35, FIN-40351 Jyväskylä, Finland

Received March 7, 2003

Single-crystal X-ray crystallography was used to determine the structures of four metallo-organic frameworks (MOFs). A dendritic tetradentate ligand (tetrakis(isonicotinoxymethyl)methane, TINM) was used with first-row transition-metal elements copper, nickel, and cobalt to synthesize MOFs with a PtS interpenetration, due to both planar and tetrahedral junctions being present in the framework. Two different polymeric complexes, **1** and **2**, were obtained from similar starting materials, TINM and $Cu(NO_3)_2 \cdot 3H_2O$, but different solvents. The use of dichloromethane in addition to methanol and water promoted the coordination of nitrate ions to the copper. With only methanol and water used as solvent, the copper atom was coordinated to water molecules instead. Compound **1** has pores going through the structure in two dimensions, along crystallographic axes *a* and *c* with diameters of the pores (the diameters correspond to the minimum distances between van der Waals surfaces of opposing walls defined by projection along channel axis) approximately 1.0×3.1 and 2.5×3.7 Å, respectively. Compound **2** has channels along all crystallographic axes. The dimensions of the channels are 3.2×3.7, 3.7×5.0, and 2.8×4.1 Å, respectively. The structures of **3** and **4** entrap a large guest ligand molecule in the framework. The guest ligand is uncoordinated, although the pattern that the entrapped guests form brings the two arms of any two guests within close range. The lack of 3-fold penetration is due to only two arms being close to each other and also the fact that there is no space for an additional set of metal centers.

Introduction

The quest for control over supramolecular structures has in the past decade created an interesting field of chemistry dealing with supramolecular, polymeric networks. These zeolite-mimicking organic or metallo-organic networks are composed of a variety of molecular tectons. The tectons, supramolecular synthons,[1] are held together by metal−ligand coordination bonds,[2,3] hydrogen bonds,[4] stacking interactions,[5] S−S bonds, metal−metal contacts, weak hydrogen bonds such as $\pi\cdots\pi$ interactions, or mixtures of these.[3,6] These networks come in many forms such as one-dimensional rods, ladders, and tubes,[7] two-dimensional grids, sheets, and honeycombs,[3] and three-dimensional diamondoid (tetrahedral centers),[4,8] cubic diamondoid, and simple cubic lattices (octahedral centers).[9,10] There are also other variations of 3-D networks, such as chiral,[11] racemic,[2] and the PtS type of networks presented in this work.[12] The PtS architecture has been thoroughly investigated by Kim et al.[12] The 3-D network architectures tend to lead to pores in the crystal

* To whom correspondence should be addressed. E-mail: Kari.Rissanen@cc.jyu.fi.

[†] E-mail: Kalle.Nattinen@cc.jyu.fi.

(1) Desiraju, G. R. *Angew. Chem., Int. Ed. Engl.* **1995**, *34*, 2311. Wang, X.; Simard, M.; Wuest, J. D. *J. Am. Chem. Soc.* **1994**, *116*, 12119. Schmidt, G. M. J. *Pure Appl. Chem.* **1971**, *27*, 647.

(2) Kheradmandan, S.; Schmalle, H. W.; Jacobsen, H.; Blacque, O.; Fox, T.; Berke, H.; Gross, M.; Decurtins, S. *Chem. Eur. J.* **2002**, *8*, 2526. Jensen, P.; Batten, S. R.; Moubaraki, B.; Murray, K. S. *J. Chem. Soc., Dalton Trans.* **2002**, 3712.

(3) Ino, I.; Zhong, J. C.; Munakata, M.; Kuroda-Sowa, T.; Maekawa, M.; Suenaga, Y.; Kitamori, Y. *Inorg. Chem.* **2000**, *39*, 4273.

(4) Ermer, O.; Lindenberg, L. *Helv. Chim. Acta* **1991**, *74*, 825. Simard, M.; Su, D.; Wuest, J. D. *J. Am. Chem. Soc.* **1991**, *113*, 4696. Venkatamaran, D.; Lee, S.; Zhang, J.; Moore, J. S. *Nature* **1994**, *371*, 591. Sauriat-Dorizon, H.; Maris, T.; Wuest, J. D. *J. Org. Chem.* **2003**, *68*, 240.

(5) Biradha, K.; Domasevitch, K. V.; Moulton, B.; Seward, C.; Zaworotko, M. J. *J. Chem. Soc., Chem. Commun.* **1999**, 1327.

(6) Tong, M.-L.; Zheng, S.-L.; Chen, X.-M. *Polyhedron* **2000**, *19*, 1809.

(7) Muthu, S.; Yip, J. H. K.; Vittal, J. J. *J. Chem. Soc., Dalton Trans.* **2002**, 4561.

(8) Hirsch, K. A.; Wilson, S. R.; Moore, J. S. *Inorg. Chem.* **1997**, *36*, 2960. Hirsch, K. A.; Wilson, S. R.; Moore, J. S. *Chem. Commun.* **1998**, 13.

(9) Yaghi, O. M.; Li, H.; *J. Am. Chem. Soc.* **1995**, *117*, 10401.

(10) Plater, M. J.; Foreman, M. R. St. J.; Skakle, J. M. S. *Cryst. Eng.* **2001**, *4*, 293. Goodgame, D. M. L.; Grachvogel, D. A.; White, A. J. P.; Williams, D. J. *Inorg. Chem.* **2001**, *40*, 6180. Hoskins, B. F.; Robson, R. *J. Am. Chem. Soc.* **1990**, *112*, 1546.

(11) Carlucci, L.; Ciani, G.; Macchi, P.; Proserpio, D. M. *Chem. Commun.* **1998**, 1837. Kepert, C. J.; Rosseinsky, M. J. *Chem. Commun.* **1998**, 31.

10.1021/ic034246r CCC: $25.00
Published on Web 07/30/2003

lattice which are usually filled with solvent molecules or anions of metal centers. Another possibility to fill the empty space left in the lattice of the 3-D networks is polycatenation, where 2 or more (currently up to 11) networks interpenetrate, resulting in a compact structure.[13] The interpenetration can also occur with sheets, with 2-D structural motifs.[14] The degree of interpenetration is generally directly related to the bridged metal−metal distance, which dictates the size of the cavities or the circumference of the rings.[3] Contrary to nature, the crystal engineer tries to maximize the empty space in the lattice to create channels or pores. The porous material can be used as a trap (or clathrate) for guest molecules,[15] in chemical sensing,[16] as light element ceramics,[17] as electronic switches, or in the storage of gases.[18,19] Until now, guests trapped in the network have been fairly small, the largest of them being *tert*-butylbenzene, 1-(4′-pyridyl)pyridin-4-one, pyrene, and benzophenone.[4,5,10] Unless they are coordinated to the metals, most of the guest molecules are not completely fixed inside the cavities and channels of the structure. The mobility of the guests manifests itself as disorder in the resulting X-ray structures. The guest inclusion can be both reversible and irreversible: some of the networks allow removal and recovery of solvents in and out of the lattice,[1,4,10,20] while the removal of guests leads to the collapse of the structure and decomposition of the crystal integrity with others.[21] The coordination networks offer attractive properties such as modularity (i.e. a large number of identical sites available), regioselectivity, stereoselectivity, shape selectivity, and exact information on the nature of binding (position in crystal lattice) as opposed to other methods such as absorption or adsorption on the surface.[22] Some claims have been made that the structure of networks could be anticipated in advance, but the majority of crystallizations lead to varying degrees of unexpected results such as two different structures from one-pot crystallization.[2] The cis and trans isomers of a ligand have also been reported to yield completely different metallo-organic frameworks (MOFs).[21]

This work deals with interpenetrated tetradentate ligand metal coordination PtS polymers with a packing similar to that of the porphyrin networks of Abrahams et al.[23] and the work of Carlucci et al.[24] with pseudo-square-planar tetradentate building blocks. Despite some examples of tetradentate ligands used in the construction of 3-D coordination networks,[4,25] most of the results are from bidentates such as 4,4′-bipyridine or tridentate ligands.[8,10,13,21,26,27] When metallic synthons are used merely as spacers, the MOF topologies are being controlled only by the organic donor units—the ligands.[28] The use of tri- or tetradentate ligands adds new variables to the toolbox of MOFs. The geometry of the branching with an organic center is not limited to those of the coordination bonds of the metals. To study the 3-D coordination networks of flexible organic tetradentate ligands and their properties, we have launched a study of tetrakis(nicotinoxymethyl)methane (TNM) and tetrakis(isonicotinoxymethyl)methane (TINM) as ligands using first- and

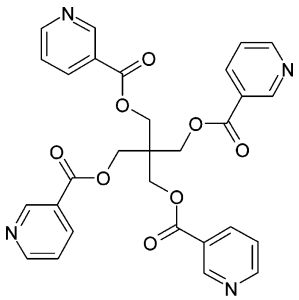

TNM

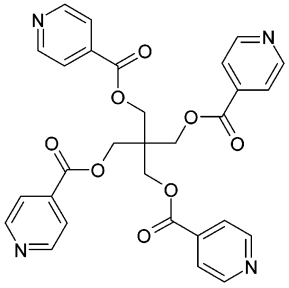

TINM

(12) Kim, J.; Chen, B.; Reineke, T. M.; Li, H.; Eddaoudi, M.; Moler, D. B.; O'Keeffe, M.; Yaghi, O. M. *J. Am. Chem. Soc.* **2001**, *123*, 8239.

(13) Hirsch, K. A.; Wilson, S. R.; Moore, J. S. *Chem. Eur. J.* **1997**, *3*, 765. Withersby, M. A.; Blake, A. J.; Champness, N. R.; Cooke, P. A.; Hubberstey, P.; Realf, A. L.; Teat, S. J.; Schröder, M. *J. Chem. Soc., Dalton Trans.* **2000**, 3261. Batten, S. R.; Harris, A. R.; Jensen, P.; Murray, K. S.; Ziebell, A. *J. Chem. Soc., Dalton Trans.* **2000**, 3829. Liu, Y.-H.; Wu, H.-C.; Lin, H.-M.; Hou, W.-H.; Lu, K.-L. *Chem. Commun.* **2003**, 60. Liu, Y.-H.; Lin, C.-S.; Chen, S.-Y.; Tsai, H.-L.; Ueng, C.-H.; Lu, K.-L. *J. Solid State Chem.* **2001**, *157*, 166. Carlucci, L.; Ciani, G.; Proserpio, D. M.; Rizzato, S. *Chem. Eur. J.* **2002**, *8*, 1519. Reddy, D. S.; Dewa, T.; Endo, K.; Aoyama, Y. *Angew. Chem., Int. Ed.* **2000**, *39*, 4266.

(14) Withersby, M. A.; Blake, A. J.; Champness, N. R.; Cooke, P. A.; Hubberstey, P.; Schröder, M. *New J. Chem.* **1999**, *23*, 573.

(15) Tong, M.-L.; Ye, B.-H.; Cai, J.-W.; Chen, X.-M.; Ng, S. W. *Inorg. Chem.* **1998**, *37*, 2645.

(16) Jung, O.-S.; Kim, Y. J.; Lee, Y.-A.; Park, J. K.; Chae, H. K. *J. Am. Chem. Soc.* **2000**, *122*, 9921.

(17) Williams, D.; Pleune, B.; Kouvetakis, J.; Williams, M. D.; Andersen, R. A. *J. Am. Chem. Soc.* **2000**, *122*, 7735.

(18) Halder, G. J.; Kepert, C. J.; Maoubaraki, B.; Murray, K. S.; Cashion, J. D. *Science* **2002**, *298*, 1762.

(19) Eddaoudi, M.; Kim, J.; Rosi, N.; Vodak, D.; Wachter, J.; O'Keefe, M.; Yaghi, O. M. *Science* **2002**, *295*, 469.

(20) Venkatamaran, D.; Gardner, G. B.; Lee, S.; Moore, J. S. *J. Am. Chem. Soc.* **1995**, *117*, 11600. Fujita, M.; Kwon, Y. J.; Washizu, S.; Ogura, K. *J. Am. Chem. Soc.* **1994**, *116*, 1151. Endo, K.; Sawaki, T.; Koyanagi, M.; Kobayashi, K.; Masuda, H.; Aoyama, Y. *J. Am. Chem. Soc.* **1995**, *117*, 8341. Mahdyarfar, A.; Harris, K. D. M. *J. Chem. Soc., Chem. Commun.* **1993**, 51.

(21) Fan, J.; Zhu, H.-F.; Okamura, T.; Sun, W.-Y.; Tang, W.-X.; Ueyama, N. *Inorg. Chem.* **2003**, *42*, 158.

(22) Gröhn, F., Kim, G.; Bauer, B. J.; Amis, E. J. *Macromolecules* **2001**, *34*, 2179.

(23) Abrahams, B. F.; Hoskins, B. F.; Michail, D. M.; Robson, R. *Nature* **1994**, *369*, 727.

(24) Carlucci, L.; Ciani, G.; Gudenberg, D. W. v.; Proserpio, D. M. *New J. Chem.* **1999**, *23*, 397.

(25) Carlucci, L.; Ciani, G.; Proserpio, D. M.; Sironi, A. *Angew. Chem., Int. Ed. Engl.* **1996**, *35*, 1088. Venkataraman, D.; Lee, S.; Moore, J. S.; Zhang, P.; Hirsch, K. A.; Gardner, G. B.; Covey, A. C.; Prentice, C. L. *Chem. Mater.* **1996**, *8*, 2030. Moore, J. S. *Nature* **1995**, *374*, 495.

(26) Carlucci, L.; Ciani, G.; Proserpio, D.; Rizzato, S. *CrystEngComm* **2002**, *4*, 121.

(27) Janiak, C. *Angew. Chem., Int. Ed.* **1997**, *36*, 1431. Gardner, G. B.; Venkatamaran, D.; Moore, J. S.; Lee, S. *Nature* **1995**, *374*, 792.

(28) Carlucci, L.; Ciani, G.; Proserpio, D. M.; Sironi, A. *Inorg. Chem.* **1997**, *36*, 1736.

second-row transition-metal ions such as cobalt, nickel, copper, zinc, and silver cation. The TNM and TINM ligands provide four sites for strong metal coordination. The capability of assuming both planar and tetrahedral conformation due to flexibility of the arms provides interesting possibilities for MOF geometries and dimensionalities. Four other lower dimensionality MOFs have also been synthesized and will be reported elsewhere.

Experimental Section

Materials and Measurements. All commercially available chemicals are of reagent grade and used as received without further purification. TINM and TNM were synthesized as previously reported.[29] The purity of products was confirmed by elemental analysis. TGA experiments were carried out at a heating rate of 5 °C/min under nitrogen. The elemental analysis was done at the University of Joensuu with a CE-Instruments EA1110 instrument.

Preparation of the Complexes. $[Cu(TINM)(NO_3)_2](H_2O)_{4.5}(MeOH)_{2.5}$ (1). In a solution of 50 mg (89.8 μmol) of TINM dissolved in a mixture of 10 mL of DCM and 20 mL of MeOH was added 21.7 mg (89.8 μmol) of $Cu(NO_3)_2 \cdot 3H_2O$ in 10 mL of water. The solution was slowly allowed to evaporate, and the crystalline solid was collected from the solution before complete evaporation of the solvents. The solid was washed with water and dried in air. Yield: 23%. **1** gives a low analysis in H and high analysis in C and N, suggestive of the loss of guest water molecules. Anal. Calcd for $C_{31.25}H_{24}CuN_6O_{21.25} \cdot 2H_2O$: C, 43.1; H, 4.5; N, 9.6. Found: C, 43.0; H, 3.8; N, 10.4.

$[Cu(TINM)(H_2O)_2](NO_3)_2(H_2O)_{10}$ (2). In a solution of 50 mg (89.8 μmol) of TINM dissolved in 30 mL of MeOH was added 21.7 mg (89.8 μmol) of $Cu(NO_3)_2 \cdot 3H_2O$ in 10 mL of water. The solution was slowly allowed to evaporate, and the crystalline solid was collected from the solution before complete evaporation of the solvents. The solid was washed with water and dried in air. Yield: 15%. Anal. Calcd for $C_{29}H_{28}CuN_6O_{16}$: C, 44.6; H, 3.6; N, 10.8. Found: C, 44.2; H, 3.8; N, 10.4. The values found correspond to the structure without solvent water.

$[Ni(TINM)Cl_2](TINM)_{0.25}(H_2O)_4$ (3). In a solution of 50 mg (89.8 μmol) of TINM dissolved in a mixture of 20 mL of MeCN and 10 mL of DCM was added 21.4 mg (89.8 μmol) of $NiCl_2 \cdot 6H_2O$ in 10 mL of MeOH. The solution was slowly allowed to evaporate, and the crystalline solid was collected from the solution before complete evaporation of the solvents. The solid was washed with water and dried in air. Yield: 100%. Anal. Calcd for $C_{29}H_{30}Cl_2N_5NiO_{14}$: C, 48.1; H, 5.1; N, 7.7 Found: C, 48.9; H, 4.3; N, 7.8.

$[Co(TINM)Cl_2](TINM)_{0.5}$ (4). In a solution of 50 mg (89.8 μmol) of TINM dissolved in 30 mL of MeOH was added 21.4 mg (89.8 μmol) of $CoCl_2 \cdot 6H_2O$ in 20 mL of MeOH. The solution was slowly allowed to evaporate, and the crystalline solid was collected from the solution before complete evaporation of the solvents. The solid was washed with water and dried in air. Yield: 20%. **4** gives a low analysis on C and N and high analysis on H, indicating leftover moisture in the structure. Anal. Calcd for $C_{21.7}H_{22}ClCo_{0.5}N_3O_8 + 2H_2O$: C, 50.4; H, 4.3; N, 8.1. Found: C, 50.9; H, 4.1; N, 8.0.

X-ray Studies. Single-crystal X-ray diffraction was done with a Nonius KappaCCD diffractometer with graphite-monochromated Mo Kα ($\lambda = 0.710\,73$ Å) radiation. Collect software was used in the measurement and DENZO-SMN in the processing of the data. The structures were solved and refined by full-matrix least squares on F^2 with the WinGX software package[30] utilizing SHELXS97[31] and SHELXL97[32] modules. Hydrogen atoms were refined by a riding model. Empirical absorption correction was performed for the compound **2**. The graphic presentations of the structures were created with the software Diamond.[33] The disordered solvent treatment SQUEEZE/BYPASS[36] was applied to the structures, but the structures with solvents modeled individually were found to give more accurate results and therefore sustained. The crystals were obtained by slow evaporation of solvent.

Results and Discussion

Synthesis. Compounds **1**−**4** were all obtained as crystalline solids by evaporation of the mixture of solvents. The crystals could be used for single-crystal X-ray analysis. The structures were further confirmed by elemental analyses and TGA measurements. Since the compounds only exist as solid crystalline materials, no NMR measurements were performed. The existence of channels in compounds **1** and **2** was confirmed by TGA. Several combinations of transition-metal cations, anions, and solvents were applied. However, the combinations of anions, metal cations, and solvents presented here were the only ones that we managed to produce 3D MOF structures of.

X-ray Single-Crystal Structures. All of the structures **1**−**4** are polymeric, interpenetrated metallo-organic frameworks. The topology of the interpenetrating networks is of the PtS type:[12] i.e., a 1:1 mixture of tetrahedral and square-planar junctions. Crystallographic parameters are given in Table 1.

Interpenetrated MOF Structure of Compound 1. Each asymmetric unit of **1** contains one Cu atom, the separate halves of the coordinated TINM, two coordinated nitrate anions, three methanol molecules, and five oxygens of water molecules. Despite the numerous hydrogen bond acceptors (ester and nitrate groups) in the structure, the third methanol molecule is disordered and was localized with a population parameter of 0.5. Four of the five oxygens of water molecules are also disordered. A model was built to describe the disorder where each of the four oxygens was split into two with the sum of the population parameters of the four amounting to a total of 3.5. The disorder was limited to the solvents and is due to the large amount of space available in the channels of the structure. The local coordination geometry around the Cu atom is octahedral, with the copper coordinated to four pyridyl nitrogens of the TINM in the

(29) Nättinen, K.; Rissanen, K. *Cryst. Growth Des.* **2003**, *3*, 339.

(30) Farrugia, L. J. *J. Appl. Crystallogr. 32*, 837.
(31) Sheldrick, G. M. *Acta Crystallogr*. **1990**, *A46*, 467.
(32) Sheldrick, G. M. SHELXL-97—A Program for Crystal Structure Refinement; University of Göttingen, Göttingen, Germany, 1997.
(33) Bergerhoff, G. DIAMOND—Visual Crystal Structure Information System; Prof. Dr. G. Bergerhoff, Gerhard-Domagk-Strasse 1, 53121 Bonn, Germany.
(34) Withersby, M. A.; Blake, A. J.; Champness, N. R.; Cooke, P. A.; Hubberstey, P.; Realf, A. L.; Teat, S. J.; Schröder, M. *J. Chem. Soc., Dalton Trans.* **2000**, 326.
(35) The diameters of the pores correspond to the minimum distances between van der Waals surfaces of opposing walls defined by projection along the channel axis.
(36) Spek, A. L. PLATON, A Multipurpose Crystallographic Tool; Utrecht University, Utrecht, The Netherlands, 1998.

Table 1. Crystallographic Parameters for Compounds **1**−**4**

	1	**2**	**3**	**4**
empirical formula	$[Cu(C_{29}H_{24}N_4O_8)(NO_3)_2]\cdot(H_2O)_{4.5}(CH_3OH)_{2.5}$ [a]	$[Cu(C_{29}H_{24}N_4O_8)\cdot(H_2O)_2](NO_3)_2(H_2O)_{10}$ [a]	$[Ni(C_{29}H_{24}N_4O_8)]\cdot(C_{29}H_{24}N_4O_8)_{0.25}(H_2O)_4$ [a]	$[Co(C_{29}H_{24}N_4O_8)Cl_2]\cdot(C_{29}H_{24}N_4O_8)_{0.5}$ [a]
formula wt	887.10	936.08	889.26	964.62
cryst color, shape	blue, blocks	blue, prisms	green, prisms	pink, prism
cryst dimens (mm)	0.1 × 0.2 × 0.35	0.3 × 0.3 × 0.5	0.08 × 0.08 × 0.08	0.25 × 0.15 × 0.12
cryst syst	orthorhombic	orthorhombic	tetragonal	tetragonal
space group	*Pbcn* (No. 60)	*Pbcb* (No.5 4)	$P4_2/n$ (No. 86)	$P4_2/n$ (No. 86)
a (Å)	19.446(4)	10.8150(2)	13.332(1)	13.4495(3)
b (Å)	25.677(5)	16.4130(3)	13.332(1)	13.4495(3)
c (Å)	15.778(3)	22.7861(5)	25.418(2)	25.4130(6)
α (deg)	90	90	90	90
β (deg)	90	90	90	90
γ (deg)	90	90	90	90
V (Å^3)	7878(3)	4044.7(2)	4517.9(6)	4596.9(2)
calcd density (Mg/m^3)	1.496	1.537	1.307	1.394
temp of collecn (K)	173	173	123	173
Z	8	4	4	4
R_{obsd}	R1 = 0.1499, wR2 = 0.2983	R1 = 0.1029, wR2 = 0.2800	R1 = 0.0807, wR2 = 0.1941	R1 = 0.0725, wR2 = 0.1832
R_{all}	R1 = 0.2482, wR2 = 0.3454	R1 = 0.1282, wR2 = 0.3104	R1 = 0.1349, wR2 = 0.2242	R1 = 0.1356, wR2 = 0.2222
GOF	1.116	1.061	1.072	1.033
θ range for data collecn (deg)	2.93−25.73	3.24−25.67	3.06−25.01	3.03−25.68
scan type	*ϕ*/*ω*, 0.5°	*ϕ*/*ω*, 1°	*ϕ*/*ω*, 2°	*ϕ*/*ω*, 1°
no. of rflns collected/unique/ cell refinement	88 811/29 157/26 642	40 163/15 079/13 751	23 067/14 844/11 050	24 826/15 903/12 355
no. of refined params	527	292	267	310
resid electron density (e/Å^3)	0.766/−0.571	0.847/−0.929	0.856/−0.367	0.514/−0.449

[a] The hydrogens could not be localized for the water and methanol molecules.

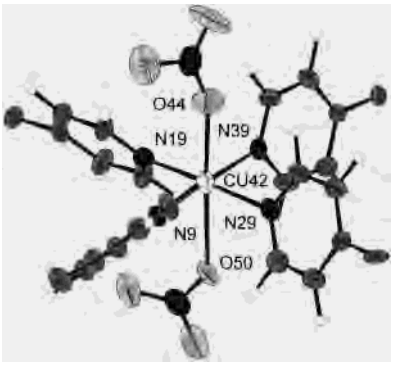

Figure 1. Coordination environment of **1**. The ellipsoids are shown at 30% probability.

equatorial plane and to two nitrate oxygens in the apical positions (Figure 1).

The pyridyl rings around the copper assume a propeller-like conformation, which is typical for heteroaromatic−metal coordination.[34] The interpenetrating matrixes of **1** are presented in Figure 2. The C−Cu−C angles (89.4−92.0°) as well as the smaller Cu−C−Cu angles (86.67−89.5°) measured from the central carbons of TINMs are close to 90°. The wider Cu−C−Cu angles are in the range of 114.8−128.1°. Three interpenetrating units of the double matrix of **1** are displayed in Figure 3.

The arrangement of the two interpenetrating matrixes with respect to each other results in channels along the crystallographic *a* and *c* axes being left in the structure. A presentation of the packing of **1** along the *a*, *b*, and *c* axes, with the solvents and anions excluded from all but the upper left corner channel of each structure, is given in Figure 4, as both as a space-filling and ball-and-stick model.

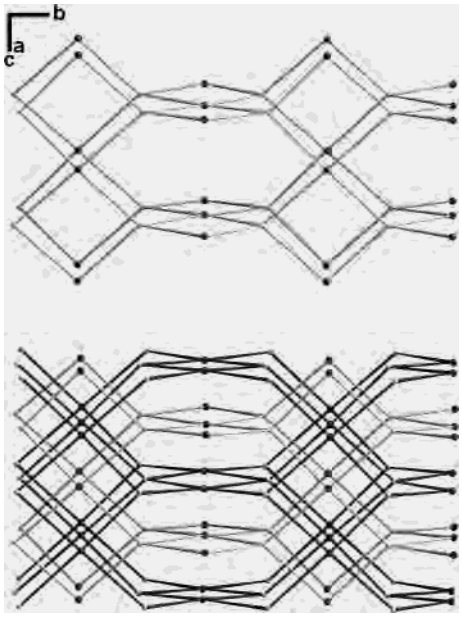

Figure 2. Interpenetrating matrixes of **1**. The central carbon (gray) and copper atoms (black) and bonds between them are displayed. In the upper part of the figure, only one of the interpenetrating matrixes of **1** is presented. In the lower part, the bonds of the second matrix are presented in dark gray.

The diameters of the pores along unit cell axes *a* and *c* are approximately 1.0 × 3.1 Å and 2.5 × 3.7 Å, respectively.[35] Calculations showed the percentage of void in the structure without solvents and anions to be 37.5%.[36]

Interpenetrated MOF Structure of Compound 2. Each asymmetric unit of **2** contains half of a Cu atom, half of a coordinated TINM, two uncoordinated nitrate anion halves, and six oxygens of water molecules, of which one (the

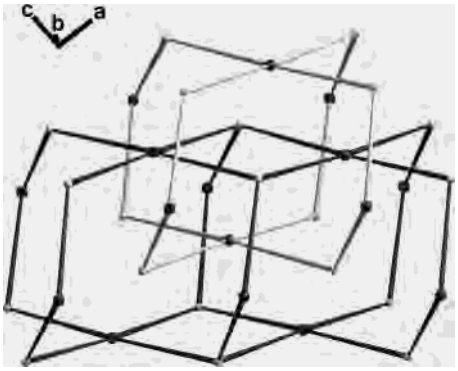

Figure 3. Three interpenetrating units of **1**. As in Figure 2, only the central carbons of TINMs (light gray) and copper atoms (black) and bonds between them are shown. The bonds of the first matrix are presented in light gray and the bonds of the second matrix in dark gray.

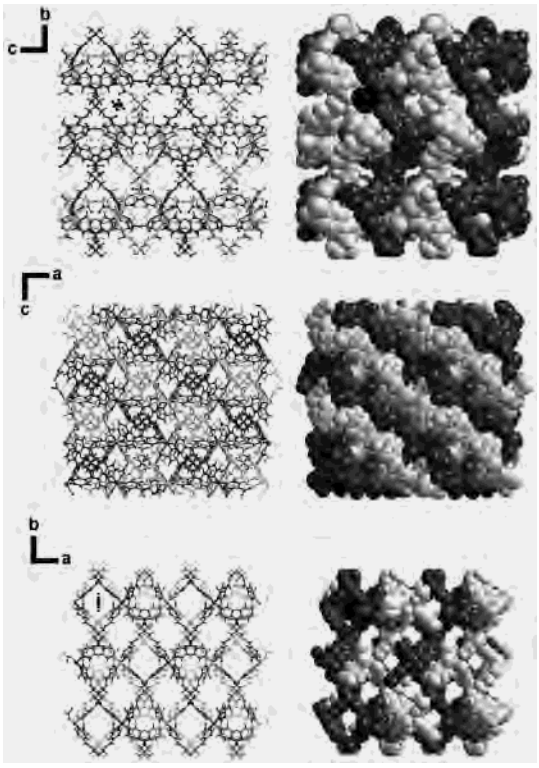

Figure 4. Parallel space-filling and ball-and-stick models for **1** along the *a*, *b*, and *c* axes. The two matrixes are displayed in light and dark gray, respectively. The solvents and anions are excluded from all but the upper left corner channel in the images of packing along the *a* and *c* axes. Solvents and anions for images of packing along the *b* axis are all excluded.

second coordinated water results from symmetry) is coordinated to the copper (Figure 5). Three of the five uncoordinated water oxygens are disordered. A model was build to describe the disorder, where two of the five uncoordinated oxygens were split into three positions and one into two positions with the total sum of the population parameters amounting to 5.0. The disorder was mainly limited to the water and is due to the large amount of space available in the channels of the structure. One carbonyl group of the TINM was also disordered and split into two positions to meet the experimental data obtained from the data collection. The packing of **2** is similar to that of **1** in its manner of interpenetration. Also, the architectures of the single matrixes

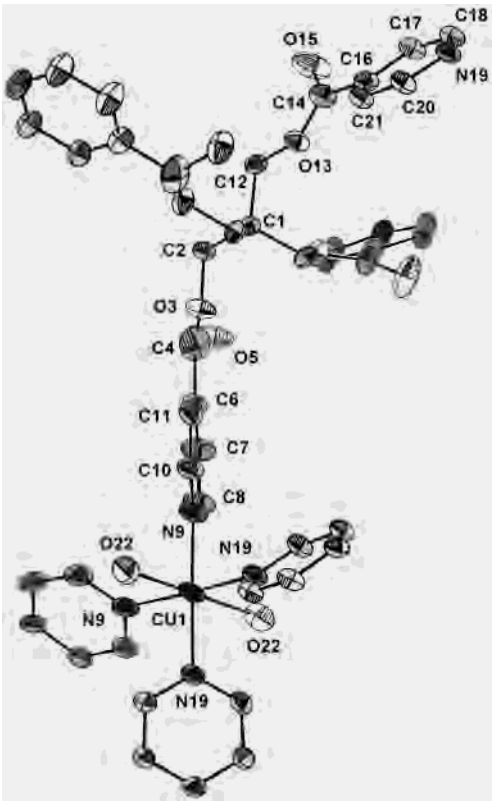

Figure 5. Coordination environment of **2**. The ellipsoids are shown at 30% probability. The asymmetric unit and the atoms coordinated to Cu1 are labeled. The disorder and hydrogen atoms are removed, and the solvent molecules are excluded.

are generally the same, with exceptions in the angles (measured from the central carbons of TINMs) of carbon−copper−carbon (55.2, 119.2, and 130.5°) and the angle between arms of the TINM (99.8−124.8°) compared to the respective angles of **1**. This inflicts a change in the size of the pores of the structure and also causes an additional set of pores to appear along the *b* axis. The ball-and-stick and space-filling models for **2** along the *a*, *b*, and *c* axes of the unit cell are presented in Figure 6. The dimensions of the channels are 3.2 × 3.7 Å, 3.7 × 5.0 Å, and 2.8 × 4.1 Å, respectively. Calculations showed the percentage of void in the structure without solvents and anions to be 39.6%.[36]

From Figure 7 it can be seen that, although there is no difference in the actual framework between the structures of **1** and **2** (the difference is in the apical coordination of the copper), the final outcome is quite different. This can be rationalized by looking at the three interpenetrating units of the matrixes of **1** and **2**. The change in the C−Cu−C angle (measured from the central carbons of the TINMs) leads to skewing of the matrix units and creation of additional channels in **2**. Although the C−Cu−C angles deviate from 90°, the copper coordination sphere remains intact: the skewing is due to the flexibility of the arms of the TINM.

Interpenetrated Ligand Entrapment MOF Structure of Compound 3. The asymmetric unit of **3** consists of half of a Ni atom, to which one Cl atom is coordinated to, a quarter of an uncomplexed TINM with a population param-

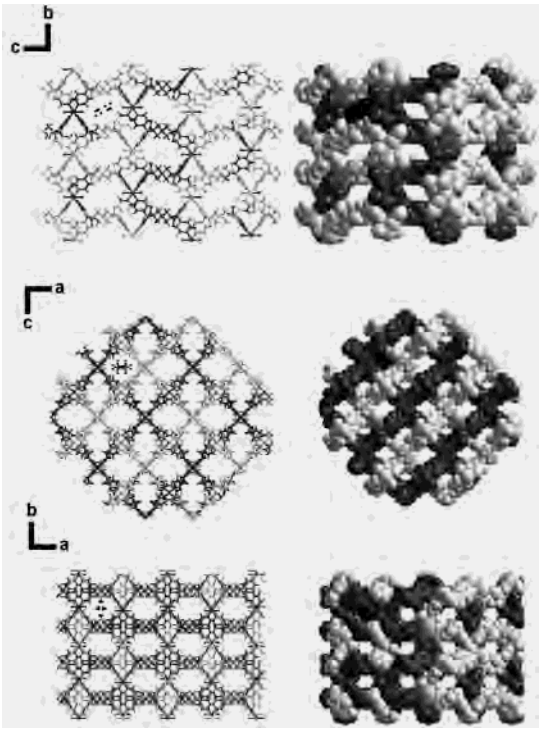

Figure 6. Parallel space-filling and ball-and-stick models for **2** along the *a*, *b*, and *c* axes. The two matrixes are displayed in light and dark gray, respectively. The solvents and anions are excluded from all but the upper left corner channel of each individual image. The disorder of the carbonyl group is removed.

eter of 0.5 (one arm, the central carbon with sof 0.125), and six solvent residual peaks sharing the space of the arm of the guest TINM (Figure 8). Due to disorder of the guest TINM, the pyridine ring of the guest was constrained to the shape of the pyridine ring of the host TINM with the constraint SAME. The solvent peaks were assigned as oxygen with the total sum of the population parameters amounting to 2.0. As with **2**, one carbonyl group of the nickel-coordinated TINM was also disordered and split into two positions to meet the data obtained from the measurement.

Generally the interpenetration of **3** follows the guidelines of **1** and **2**. However, compared to **1** and **2**, the matrixes of **3** are slightly displaced, to allow the inclusion of the uncomplexed ligand (Figure 9). The C−Cu−C angles (87.3−93.1°) as well as the smaller Cu−C−Cu angles (92.4−93.1°) measured from the central carbons of the TINMs are, like those of **1**, close to 90°. The wider Cu−C−Cu angles are all 118.4°. The narrow and wide N−C−N angles for the guest are 86.6 and 122.0°, respectively.

The guest TINM organizes in a manner that, if all the positions available for the uncomplexed ligand were filled by it (the population parameter for the uncomplexed ligand in **3** is 0.5), it could make coordination bonds to a suitable metal. The terminal nitrogens of the guest "network" are only 3.87 Å apart from each other. However, there are only two available guest arms within a coordination distance. A metal atom with two coordination sites and a tendency to tetrahedral coordination positioned between these nitrogens could result in an N−M coordination with an N−M bond length equaling 2.37 Å. Given the flexibility of the TINM, a suitable selection of metal could in principle turn the twofold interpenetration into a threefold, heterometallic one. The fact that the opposing (hindered) central carbon atom of the coordinating TINM is only 4.9 Å away from the nitrogen of the guest TINM nitrogen prevents this sort of bond formation and explains why a threefold network was not formed even in **1** and **2**, where a metal atom (copper) capable of tetrahedral coordination was used. The trapping of the uncoordinated ligand into the framework is probably due to weak interactions between the components as well as complementarity of the ligand with the framework. Competition for the available sites between the solvent and the guest TINM probably explains why only half of the sites were occupied by TINM in the framework of **3**. Calculations showed the percentage of void in the structure of **3** without solvents and anions to be 27.4%.[36,37] As expected, the percentage is lower than in the structures of **1** and **2**, since the guest ligand fills a part of the void.

Interpenetrated Ligand Entrapment MOF Structure of Compound 4. The asymmetric unit of **4** is isomorphous with that of **3** with respect to the MOF, but not with respect to the guest (Figure 10). The major difference between **3** and **4**, besides the different metal, is that the guest is not disordered and that it has a population parameter of 1.0. As with **2**, one carbonyl group of the cobalt-coordinated TINM was also disordered and split into two positions to meet the

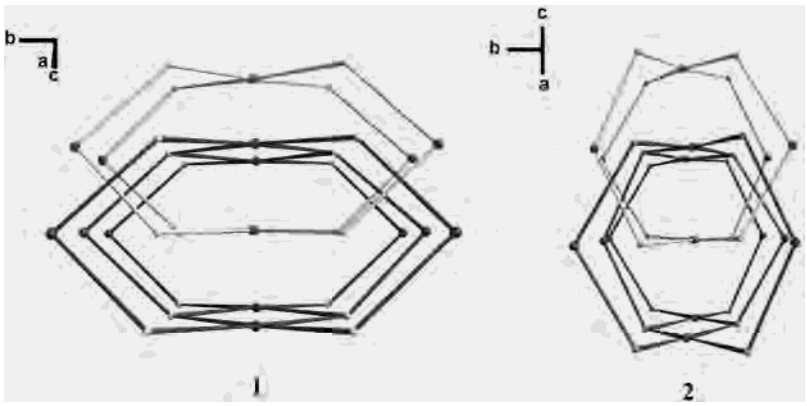

Figure 7. Perspective diagrams of three units of **1** and **2**, seen along the "tube" formed by the lower two units. The two separate matrixes are presented in light and dark gray, respectively. Only the copper and central carbon atoms of the TINMs are presented for clarity.

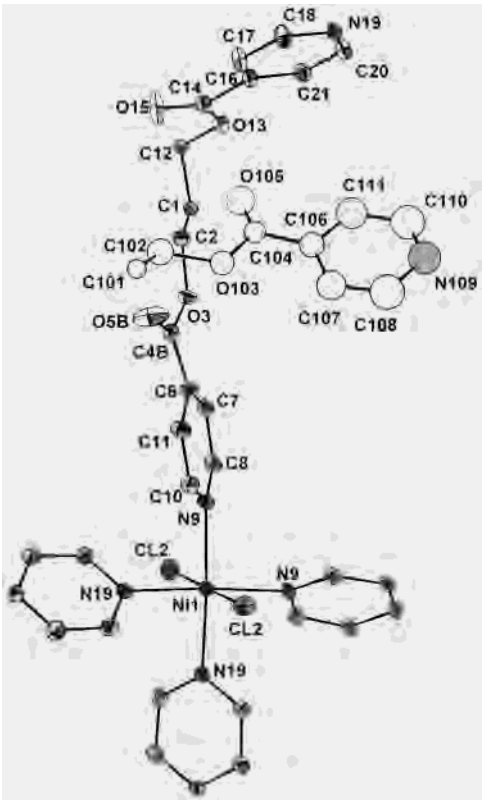

Figure 8. Coordination environment of **3**. The ellipsoids are shown at 30% probability. The asymmetric unit and the atoms coordinated to Ni1 are labeled. The disorder and hydrogen atoms are removed, and the solvent molecules are excluded. The atoms of the guest ligand are shown as spheres.

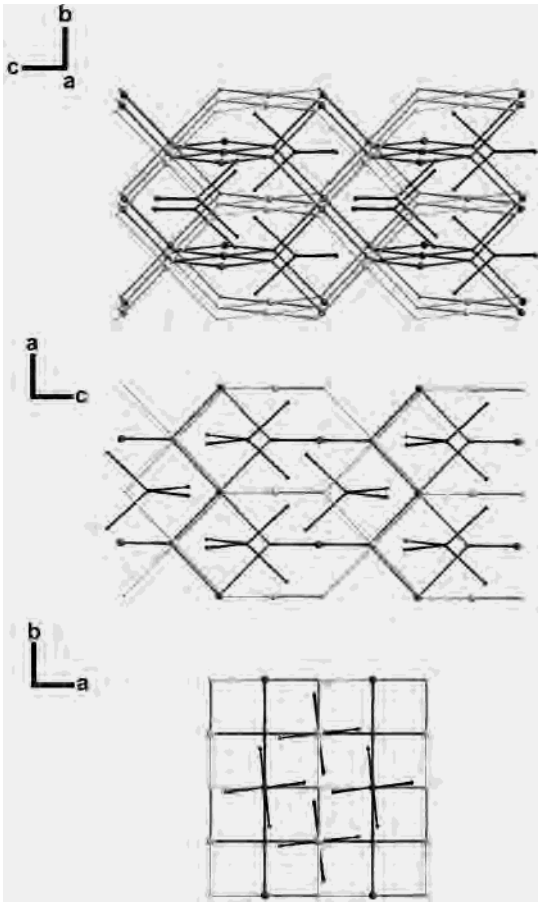

Figure 9. View of the double-matrix guest inclusion MOF **3** along the unit cell axes. The view along axis *a* is slightly turned to visualize the interpenetration. Only the nickel and central carbon atoms of the TINMs are presented. The two matrixes are displayed in light and dark gray, respectively, the entrapped ligand is displayed in black, and the solvent atoms are excluded.

experimental data obtained from the data collection. The C−Cu−C and Cu−C−Cu angles (86.8 and 92.9°) as well as the smaller Cu−C−Cu angles (92.9−93.5°) measured from the central carbons of TINMs are, like those of **1** and **3**, close to 90°. The wider Cu−C−Cu angles are all 118.2°. The narrow and wide N−C−N angles for the guest ligand are 86.3 and 122.2°, respectively. The terminal nitrogens of the guest network are only 3.96 Å apart. However, as in the structure of **3**, the 3-fold interpenetration is not possible due to lack of space for the additional metal center. In Figure 11 the cobalt, the central carbon atoms of the framework TINM, and the central carbons and nitrogens of the pyridyl rings of the four guest TINMs of three units of the interpenetrating matrixes and the four included guests of **4** are presented.

Figure 12 displays how the ligand is entrapped in the double matrix. For clarity, not all ligands of the matrixes are presented in their entirety.

As in **3**, the accommodation of the guest ligands in **4** is provided by the slight displacement (compared to **1** and **2)** of the two matrixes with respect to each other. The formation of the structure can also be seen as the guest ligand templating the buildup of the structure which, without it,

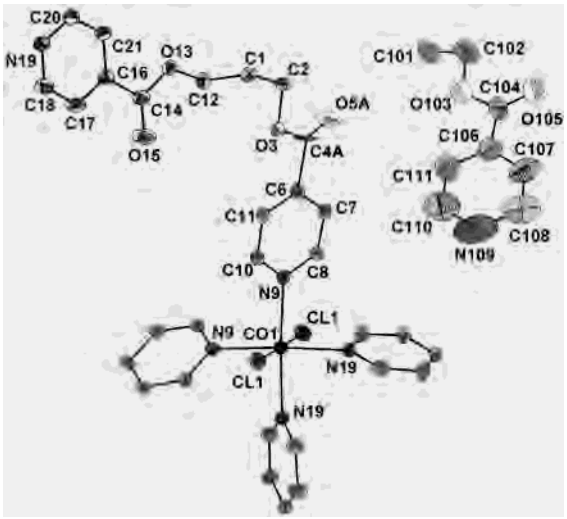

Figure 10. Coordination environment of **4**. The ellipsoids are shown at 30% probability. The asymmetric unit and the atoms coordinated to Co1 are labeled. The disorder and hydrogen atoms are removed.

might have been left too hollow and unstable. However, in compound **3** the solvent seems to be able to provide enough support for the structure by filling every second available position of the guest. Calculations showed the percentage of void in the structure of **4** without solvents and anions to

(37) The amount of void in the structure of **3** with the guest ligand with population parameter 0.5 was obtained by calculating the void for the structure **3** with the solvents and anions excluded (*a*, 8.4%) and then with the solvents, anions, and the guest ligand excluded (*b*, 46.3%). The formula $a + (b - a)/2$ gives an approximate value for the amount of void in **3**.

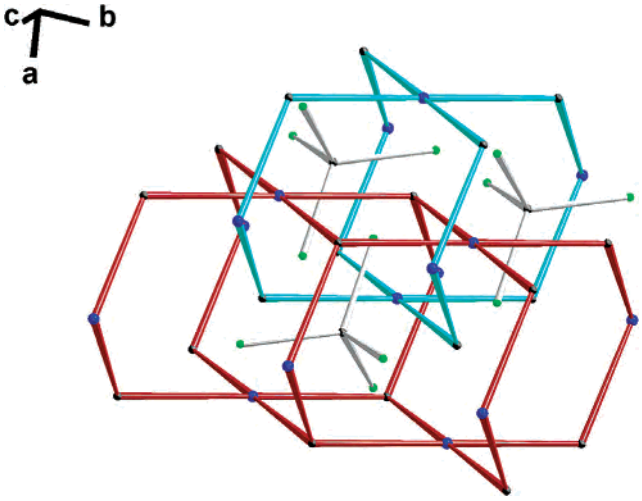

Figure 11. A diagram of the double matrix of **4** with the cobalt, central carbon atoms of the framework TINM and the central carbons and nitrogens of the pyridyl rings of the four guest TINMs presented. Three units of the interpenetrating matrixes and the four included guests of **4** are presented.

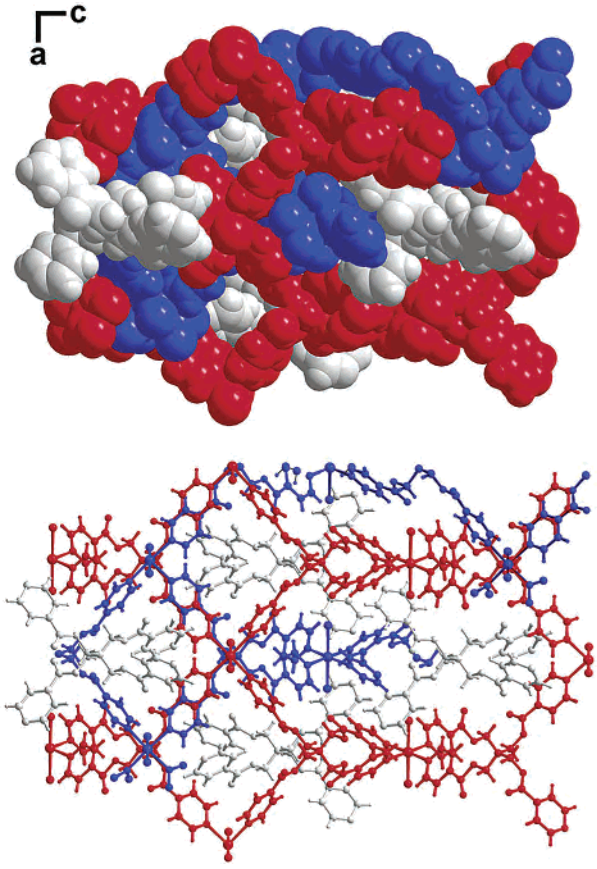

Figure 12. Space-filling and ball-and-stick presentations of the ligand entrapment in the double matrix along the crystallographic *b* axis. The ligand is presented in light gray, and the two separate matrixes are presented in red and blue, respectively. The disorder is excluded.

be 10.2%,[36] which is in agreement with the fact that the ligand consumes most of the void in **4**.

Figure 13 shows how the C−C (between two central carbons of the TINM), metal−metal, and metal−C (central C of TINM) lengths and the separation of the two matrixes are measured. These data are summarized in Table 2.

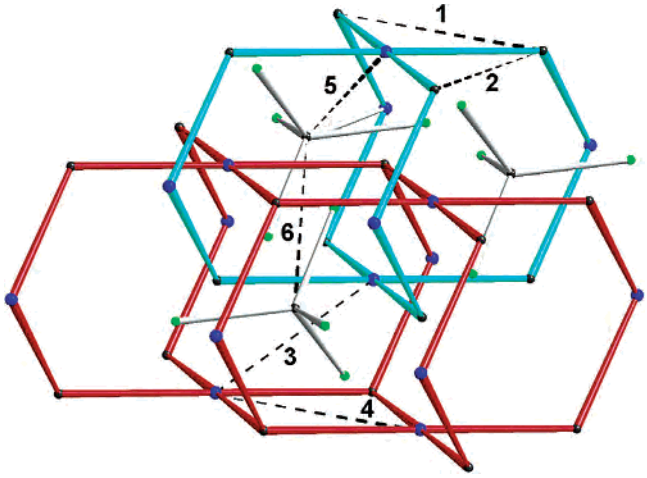

Figure 13. Definitions of the inter- and intramatrix distances of **1**−**4**.

Table 2. Intra- and Intermatrix Distances Shown in Figure 13

	compd			
distance	**1**	**2**	**3**	**4**
1	12.537(2)	15.352(38)	13.332(1)	13.422(5)
2	12.961(3)	8.223(4)	12.709(1)	12.693(2)
3	9.961(2)	10.815(5)	11.029(3)	11.11(3)
4	12.521(2)	15.73(4)	13.332(1)	13.422(5)
5			10.053(3)	10.10(3)
6			15.824(1)	15.85(4)

The skewing of the square metal coordination can be seen from distances 1 and 2 in Table 2. In compound **1**, the distances 1 and 2 are nearly equal, while in compound **2** the ratio of these distances is 2:1. In compounds **3** and **4**, the inclusion of the guest ligand results in a small increase of the intermatrix separation, the distance numbered 3 in Figure 13 and Table 2. The complementarity of the guest and the host matrix explains the smallness of the change in the MOF architecture.

Removal of Guest Molecules: TGA Studies. The thermogravimetric analyses of compounds **1**−**4** show that the structures **1** and **2** contain open channels which allow the removal of solvents. This can be seen as a step in the TGA curves of **1** and **2**, corresponding to the amount of solvents in the structures. The measured 14% and 16% weight loss when compared to the calculated 18% and 19% of solvent weight can be attributed to the slow removal of solvents during the air drying of the material and the loss of some additional solvent already in the beginning of the heating in TGA. It is noteworthy to see that the solvents were not removed before 220 °C. This might be due to the small diameter of the channels compared to the size of the solvents.[38] The decomposition of the structures of **1** and **2** occurs immediately after the removal of the solvents (Figure 14).

The solvents support the structure by interactions within the matrixes. Their removal leads to the weakening of the matrix structure and eventually its decomposition. The difference between structures **1** (nitrate anions coordinated to the copper) and **2** (water molecules coordinated to the

(38) Ewans, O. R.; Wang, Z.; Ziong, R.-G.; Foxman, B. M.; Lin, W. *Inorg. Chem.* **1999**, *38*, 2969.

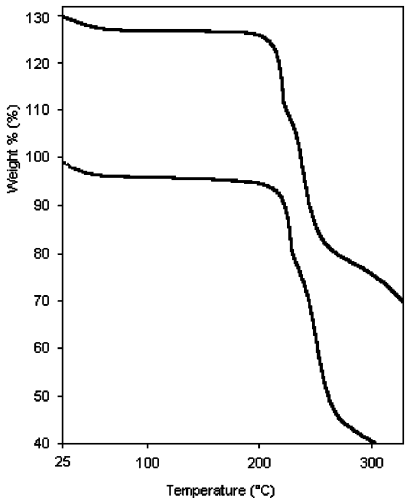

Figure 14. TGA curves for **1** (bottom) and **2** (top). For clarity, the curve of compound **2** has been shifted up by 30% in percent weight.

copper) not being visible in TGA may be due to the weak coordination of the nitrate anions and water molecules to the copper. The Cu−O distances vary in the range of 2.35−2.58 Å. The stronger Cu−N coordination bonds have bond lengths close to 2.0 Å.

The TGA study of compound **3** is consistent with what can be seen in the X-ray structures: since there are no open channels in the structure of **3**, the solvent cannot leave the lattice before the collapse of the structure at 350 °C. Compounds **3** and **4** were also not stable in air—the decomposition of the material could be observed by eye as the loss of crystal integrity and, with **4**, eventually a change of color from pink to blue. Compound **4** contains no inclusion of solvent. Therefore, the decomposition of **4** is possibly due to a phase transition.

Elemental Analysis. The elemental analyses of both **1** and **2** suggest a loss of solvent during the inevitable period of storage before the elemental analyses. The complete loss of the solvents from **2** which can be observed from EA results is probably due to collapse of the structure. TGA studies were done immediately after a short period of drying the compounds in air. This explains the presence of water in both compounds in TGA and its absence in EA. Compound **4** obviously contained moisture, which amounted to two water molecules per mole of **4**. Standard drying under vacuum prior to EA was not done due to the probable decomposition of the MOFs.

Conclusions. The compounds **1**−**4** display a uniform series of PtS interpenetrating metallo-organic frameworks. This interpenetration is due to a mixture of square-planar and tetrahedral junctions. The compounds **3** and **4** are isomorphic and display a different alignment of their matrixes with respect to each other when compared to the alignment of **1** and **2**. The main difference between **1** and **2** is in the copper coordination. Compound **1** has coordinated nitrate anions and orthogonal square-planar coordination of the pyridine ligands. In compound **2** the water molecules are coordinated to the copper atom. This results in skewed-planar coordination around the copper atom. Where compounds **1** and **2** form multidimensionally porous, solvent-including metallo-organic frameworks, compounds **3** and **4** present a guest inclusion of a large organic molecule, i.e., the ligand TINM, which is trapped uncoordinated inside the framework. The structure of **3** contains guest TINM only in every second available position, whereas all available positions of **4** are filled with guest ligand. The guest ligands are templated to a pattern which resembles the framework of the coordinated TINM. In this pattern, only two arms of the guest TINM come to a close enough distance to coordinate to a metal center. However, due to a lack of space for the metal center, the guest remains uncoordinated and the 3-fold interpenetration does not occur. In **3** and **4**, the guest ligand can also be seen as a template helping in the formation of the structures by supporting the framework and filling the space that would otherwise have been filled with less rigid solvent molecules. A loss of the inclusion solvents at 220 °C was observed in the TGA studies. The loss is not reversible—it is immediately followed by the decomposition of the structure in both compounds.

Acknowledgment. K.N. thanks the Graduate School of Bioorganic Chemistry for financial support. K.R. thanks the Finnish Academy (Project No. 777871) for financial support.

Supporting Information Available: Crystallographic data as CIF files for the compounds discussed in this paper. This material is available free of charge via the Internet at http://pubs.acs.org. The files CCDC 205507−205510 also contain the supplementary crystallographic data for this paper. These data can be obtained free of charge via www.ccdc.cam.ac.uk/conts/retrieving.html (or from the Cambridge Crystallographic Data Centre, 12 Union Road, Cambridge CB21 EZ, U.K., fax (+44) 1223-336-033, e-mail deposit@ccdc.cam.ac.uk).

IC034246R